Cite this: *Chem. Commun.*, 2011, **47**, 4108–4110

www.rsc.org/chemcomm

**COMMUNICATION**

# Facile, fast, and inexpensive synthesis of monodisperse amorphous Nickel-Phosphide nanoparticles of predefined size†

**Karl Mandel,[ac] Frank Dillon,[a] Antal A. Koos,[a] Zabeada Aslam,[a] Kerstin Jurkschat,[a] Frank Cullen,[a] Alison Crossley,[a] Hugh Bishop,[a] Karsten Moh,[b] Christian Cavelius,[b] Eduard Arzt[b] and Nicole Grobert*[a]**

***Received 23rd July 2010, Accepted 15th February 2011***
**DOI: 10.1039/c0cc02769c**

**Monodisperse, size-controlled Ni–P nanoparticles were synthesised in a single step process using triphenyl-phosphane (TPP), oleylamine (OA), and Ni(II)acetyl-acetonate. The nanoparticles were amorphous, contained ~30 at% P and their size was controlled between 7–21 nm simply by varying the amount of TPP. They are catalytically active for tailored carbon nanotube growth.**

Various synthesis routes for the production of nanoparticles were reported in recent years. These include wet-chemical techniques,[1] sonochemistry,[2] physical approaches such as ball milling[3] and various other techniques.[4] Unfortunately, these methods are relatively expensive and time consuming. For Ni–P nanoparticles to become viable for industrial applications controllable, reliable, facile, and economical production methods are essential. Only then can applications in fields such as catalysis, where Ni–P exhibits the highest activity for the hydrodesulfurization and hydrodenitrogenation[5,6] of petroleum, be achieved.

The majority of previous reports on nanoparticles derived from Ni precursors focused on thermally decomposing multiple stabilising agents to form mondisperse nanoparticles.[7] The size of the nanoparticles was typically varied by using expensive phosphanes such as trioctylphosphane (TOP), trioctyl-phosphane oxide (TOPO) and oleic acid.[8–10] With these methods, crystalline Ni particles were obtained. More recently size-controlled crystalline Ni nanoparticles were produced by varying the amount of only one stabilizing agent.[10] The influence of oleylamine (OA) and TOP was systematically studied and the amount of TOP was seen to control the size of the nanoparticles. Only a few reports can be found on Nickel-Phosphine nanoparticles. Recently, hollow $Ni_2P$ particles, exhibiting the Kirkendall effect were reported[11] and size control of the voids was achieved.[12] Further, amorphous $Ni_2P$ particles were reported using a synthesis temperature of 240 °C. Heating the particles to 300 °C lead to the formation of hollow, crystalline $Ni_2P$ particles.[13] Amorphous Ni–P nanoparticles are interesting as their amorphous nature may lead to different properties, such as enhanced catalysis,[14] due to their low range ordered structure.

Here a simple one-pot, one-step approach is described. The method involves only three reagents; namely 1 mmol Ni(II)acetylacetonate ($Ni(acac)_2$), x ml oleylamine (OA), and y mmol triphenylphosphane (TPP). The reagents were placed into a three neck flask equipped with a magnetic stirrer and a reflux cooler as well as with a thermometer which directly measured the temperature of the liquid. The flask was flushed with Ar for 10 min whilst stirring at room temperature before the temperature was raised at a heating rate of 17 °C $min^{-1}$ to 220 °C. Typically, at 215 °C, the solution turned from green to black, indicating the formation of nanoparticles. After only 10 min the heating mantle was removed and the solution was allowed to cool to room temperature under stirring. The nanoparticles were collected by adding an excess of ethanol, centrifuging at 1520 g and, after removal of the liquid phase, the nanoparticles could easily be re-dispersed in cyclo-hexane. Details on initial experimental studies performed using different combinations of oleylamine and oleic acid, can be found in the supplementary information.

Transmission electron microscopy (TEM) studies revealed that by varying the ratio of OA to TPP the nanoparticle size could be controlled. Fig. 1 depicts nanoparticles produced using 3 ml OA in conjunction with 10, 20, 30 and 40 mmol TPP, respectively.

It was found that the size of the nanoparticle depends linearly on the TPP concentration and ranges from 7–21 nm, *i.e.* 7 nm nanoparticles were produced using 40 mmol TPP, 11 nm using 30 mmol, 16 nm using 20 mmol, and 21 nm using 10 mmol. An upper size limit was reached for $<6$ mmol TPP where macroscopic aggregates formed. Therefore, the variation of the amount of TPP enables size selection of the nanoparticles. In order to demonstrate size selection the amount of OA was kept constant at either 3 ml or at 20 ml (Fig. 2). The same trend in nanoparticle size applies to samples synthesised using higher oleyamine contents, *e.g.* 20 ml (60 mmol). Hence, the size of the particles depends on the amount of TPP but not significantly on the amount of OA.

[a] *Department of Materials, University of Oxford, Parks Road, Oxford, OX1 3PH, UK*
[b] *INM-Leibniz-Institute for New Materials, Campus D2 2, 66123 Saarbrücken, Germany*
[c] *Faculty of Physics, University of Ulm, Albert-Einstein-Allee 1, 89081 Ulm, Germany*

† Electronic supplementary information (ESI) available. See DOI: 10.1039/c0cc02769c

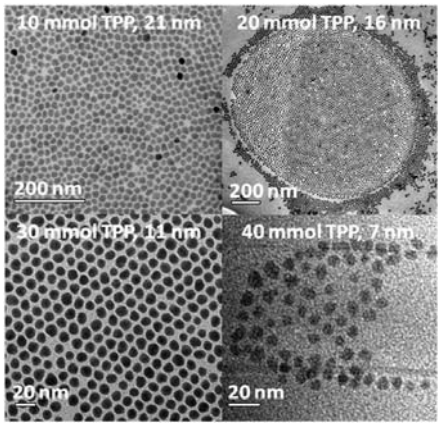


**Fig. 1** TEM images of nanoparticles produced using 3 ml OA in conjunction with 10, 20, 30, and 40 mmol TPP respectively. Variation of the particle size (21 nm, 16 nm, 11 nm, 7 nm) was achieved by changing the TPP content.

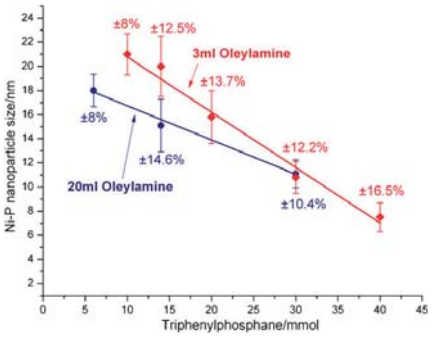


**Fig. 2** Size of Ni–P nanoparticles as function of the TPP concentration. Standard deviation of the particle size of each sample in percent.

All Ni–P nanoparticle samples exhibit an amorphous structure, no peaks for crystalline Ni or Ni–P could be identified by XRD. The amorphous nature of the nanoparticles was also confirmed by electron diffraction (see inset Fig. 3). Moreover, no crystalline order of the nanoparticles could be observed using high-resolution TEM. However, it appears that smaller (*ca.* 2 nm) crystalline seed nanoparticles were present (bottom right hand side corner in Fig. 3).

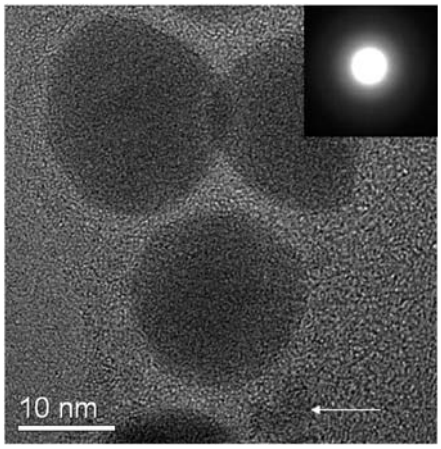


**Fig. 3** High-resolution TEM image of the Ni–P nanoparticles (6 mmol TPP). The arrow indicates a seed crystal formed during the decomposition process. The inset shows the diffraction pattern and the amorphous nature of the nanoparticles.

XPS analyses were performed in order to analyse the chemical nature of the nanoparticles. From the Ni 2p3/2 peak it was observed that Ni (853 eV[15]) as well as Ni oxide (857.2 eV[16]) were present (see Fig. 4A). The Ni oxide was present as a thin layer on the nanoparticles which formed upon exposure of the nanoparticles to air contact. Ion bombardment was used to ablate the oxide layer and the organic capping. After this treatment for 3 and 5 min, the O 1s peak vanished along with the oxide peaks of P 2p3/2 (134 eV[17]) and Ni 2p3/2 (Fig. 4A and B). Even after 5 min of ion bombardment of the nanoparticles surface, P (129.5[17]) (Fig. 4B) was still present. Careful peak fitting of the XPS data revealed a slight shift of the P 2p3/2 peak position from 130.3 eV, (graph 1 in Fig. 4B) to 129.5 eV (graph 2 and 3 in Fig. 4B) after ion bombardment. A binding energy of 130.3 eV can be associated with organically bound phosphorous, as in TPP.[17]

The incorporation of P in the Ni nanoparticles explains their amorphous nature as previous studies observed the formation of amorphous Ni nanoparticles (using a different synthesis route) when the P content was higher than 10 mol%.[18] Further, the formation of a Ni–P glass might have occurred, which is reported to be stable between 12.5–25 at% P for bulk samples.[19] An estimation from the XPS peaks of P and Ni indicates a P content of around 30 (±5) at%. The P content was the same for all nanoparticle sizes formed (Fig. 2) and was confirmed by EDX analysis of the particles.

Annealing of our particles under inert atmosphere and subsequent measurement with XRD resulted in peaks corresponding to NiO, where an oxidation of Ni probably occurred

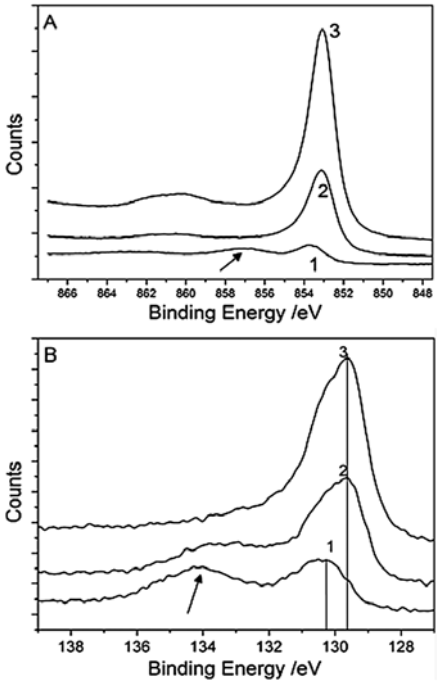


**Fig. 4** XPS. (A) Ni peak: The change of peaks from graph 1 (no ion bombardment) to graph 2 (after 3 min of ion bombardment) to graph 3 (after five minutes of ion bombardment) indicates the removal of Ni oxide (arrow). (B) P 2p3/2 peak shows initial oxidation of P (graph 1, left hand side peak, arrow). However, the O could be removed partly after 3 min (graph 2) and totally after 5 min of ion bombardment (graph 3). The P peak shift from 130.2 eV (graph 1) fitting for P in TPP to 129.5 eV (graph 2 and 3) fitting for pure P suggests incorporation of P in the particles.

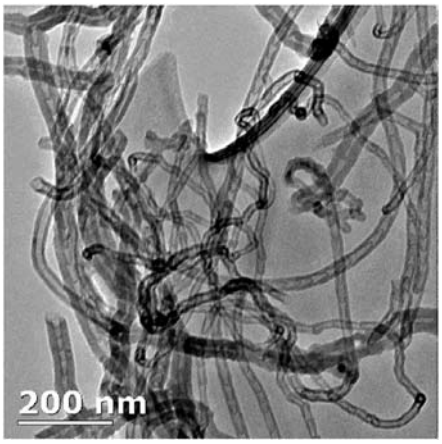


**Fig. 5** TEM image of CNTs, grown from Ni–P particles. The majority of the CNTs formed exhibited compartmentalised sections, also described as bamboo structure.

during air contact of the particles during the XRD measurement. Therefore it is unlikely that the stoichiometric compound $Ni_2P$ was formed as annealing of those particles resulted in the formation of crystalline $Ni_2P$.[13]

The particles appear to be stabilised by TPP and not OA. However, OA plays an important role in nanoparticle formation by forming a $(Ni(acac)_2)$–OA adduct as proposed previously.[8] Only a molar ratio of 2 : 1 OA : $(Ni(acac)_2)$ or larger resulted in the formation of a green complex during reaction in our experiments. Without the preformed complex, no nanoparticle formation was observed. Although OA plays a crucial role in the formation of the nanoparticles the variation of the amount of OA only slightly influences the size of the nanoparticles. As no other solvents were added, the reason for the slight variation might be due to the different concentration of the nanoparticles per absolute amount of liquid in the flask. This problem was previously avoided by using a constant amount of liquid by adding a solvent.[9] Herein no additional reagents were added in order to keep the process as simple as possible and to avoid further unknown chemical interactions of solvents with the stabilising agents and precursor. Different stabilising agents influence the size of the nanoparticles due to their different steric demand.[8] In particular it was shown that amount of TPP systematically influences their size.

Homogeneous size controlled Ni–P nanoparticles play an important role in catalytic processes. For example, the industrial scale production of structurally well-defined carbon nanotubes (CNT) relies on the fast, facile, and inexpensive production of size-controlled metal nanoparticles. Hence, preliminary CNT growth experiments were carried out using the as produced Ni–P nanoparticles in conjunction with toluene in a tube furnace at 800 °C under ambient conditions in an Ar atmosphere. As a result it was confirmed that size control over nanotube diameters can indeed be achieved by using nanocatalyst particles of predefined size. Fig. 5 shows a representative TEM micrograph of the CNTs produced. The size distribution of the nanotubes is shown in the supplementary information along with a representative Raman spectre of the tubes. Some deviations of the CNT from the nanoparticle diameters were observed, indicating partial coalescence of the particles during the synthesis process. The majority of the CNTs formed exhibited compartmentalised sections, also described as bamboo structure.

A simple and fast one pot approach to produce amorphous Ni–P nanoparticles by using only three—comparably inexpensive—chemicals, without additional reducing agents or solvents was reported. Monodisperse nanoparticles were produced by keeping the reagents at 220 °C for only 10 min—which is much shorter in time than typical approaches where high temperatures are often kept for more than an hour. Whilst the different steric demand of capping molecules controls the size of particles, the abundance of a capping agent can also control the nanoparticles size as it might at an earlier stage after their nucleation block subsequent growth. The size of the nanoparticles can hence be controlled by changing the amount of the cheap phosphane TPP. The process described here proved to be very versatile and it is likely to be applicable to other transition metals, investigations into which are currently under way. It was also shown that size controlled nanoparticles are indeed suitable in order to control the production of tailored CNTs.

We thank Paul Ziemann, Faculty of Physics, University of Ulm, for fruitful discussions and Chris Salter (BegbrokeNano, University of Oxford) for SEM-EDX analysis. We gratefully acknowledge Evonik Industries (KM), Studienstiftung d. dt. Volkes (KM). This work has also been supported by the Royal Society (NG), the European Commission under the 6 Framework Programme (STREP project BNC Tubes, Contract Number NMP4-CT-2006-033350) (NG), and the ERC Starting Grant (ERC-2009-StG-240500) (NG).

## Notes and references

1 H. Bönnemann and R. M. Richards, *Eur. J. Inorg. Chem.*, 2001, **10**, 2455–2480.
2 A. Gedanken, *Ultrason. Sonochem.*, 2004, **11**(2), 47–55.
3 A. K. Singh and O. N. Srivastava, *J. Alloys Compd.*, 1995, **227**(1), 63–68.
4 B. L. Cushing and V. L. Kolesnichenko, *Chem. Rev.*, 2004, **104**(9), 3893–3946.
5 S. Ted Oyama, *J. Catal.*, 2003, **216**, 343–352.
6 Y. Shu and S. Ted Oyama, *Carbon*, 2005, **43**, 1517–1532.
7 S. Sun and H. Zeng, *J. Am. Chem. Soc.*, 2004, **126**(1), 273–279.
8 J. Park and E. Kang, *Adv. Mater.*, 2005, **17**(4), 429–434.
9 S. Carenco and C. Boissiere, *Chem. Mater.*, 2009, **22**(4), 1340–1349.
10 F. Davar and Z. Fereshteh, *J. Alloys Compd.*, 2009, **476**(1–2), 797–801.
11 R.-K. Chiang and R.-T. Chiang, *Inorg. Chem.*, 2007, **46**(2), 369–371.
12 X. Zheng and S. Yuan, *Mater. Lett.*, 2009, **63**, 2283–2285.
13 J. Wang and A. C. Johnston-Peck, *Chem. Mater.*, 2009, **21**, 4462–4467.
14 T. Burchardt and V. Hansen, *Electrochim. Acta*, 2001, **46**, 2761–2766.
15 L. Salvati L and L. E. Makovsky, *J. Phys. Chem.*, 1981, **85**, 3700.
16 S. O. Grim and L. J. Matienzo, *J. Am. Chem. Soc.*, 1972, **94**, 5116.
17 J. F. Moulder, *Handbook of X-ray Photoelectron Spectroscopy*, Perkin Elmer Corporation, Minesota, 1979.
18 S. Xie and M. Qiao, *J. Phys. Chem. B*, 2005, **109**(51), 24361–24368.
19 D. Tatchev and Ts. Vassilev, *J. Non-Cryst. Solids*, 2010, **356**, 351–357.

 